Scanning Electrochemical Microscopy. 27. Application of a Simplified Treatment of an Irreversible Homogeneous Reaction following Electron Transfer to the Oxidative Dimerization of 4-Nitrophenolate in Acetonitrile

David A. Treichel, Michael V. Mirkin,† and Allen J. Bard*

Department of Chemistry and Biochemistry, The University of Texas at Austin, Austin, Texas 78712

Received: February 16, 1994®

Scanning electrochemical microscopy (SECM) was employed to study the rate of the second-order homogeneous reaction of a species electrogenerated at an ultramicroelectrode tip. Oxidation of 4-nitrophenolate in acetonitrile to the phenoxyl radical took place at a gold ultramicroelectrode (5-μm diameter) held in close proximity to a larger substrate electrode that detected the tip-generated species. A radical dimerization rate constant of 1.2 (±0.3) × 10^8 M^{-1} s^{-1} was determined. Approximate analytical equations for the treatment of irreversible kinetics following electron transfer were developed to simplify the analysis of feedback and collection data for both first- and second-order reactions. The effect of possible interference by the reference material added to allow precise determination of the tip–substrate spacing (benzoquinone or ferrocene) was also investigated.

Introduction

The scanning electrochemical microscope (SECM)[1-3] has been shown to be useful in studies of the kinetics of first- and second-order homogeneous reactions associated with electrode processes.[4-6] The principle of such measurements is shown in Figure 1. An ultramicroelectrode (tip) is held in close proximity to a conductive substrate electrode with the solution in the interelectrode gap and surrounding the electrodes containing electroactive species R. A counterelectrode and a reference electrode are located in the bulk solution, and the potentials of the tip and substrate electrodes are controlled with a bipotentiostat at levels where the reactions

$$R \rightarrow O + ne \quad \text{(tip)} \tag{1}$$

$$O + ne \rightarrow R \quad \text{(substrate)} \tag{2}$$

occur at diffusion-controlled rates. In the absence of decomposition of tip-generated species O, essentially all of it is collected by the substrate electrode, i.e., the substrate current, i_S, essentially equals the tip current, i_T. This leads to a feedback to the tip that causes i_T to be larger than the value found with the tip far from the substrate ($i_{T,\infty}$).[1-3] When O is consumed in a reaction

$$O \xrightarrow{k_c} \text{products (gap)} \tag{3}$$

both the collection and the feedback currents are smaller than the values found in the absence of this reaction, and a consideration of the change in $|i_S/i_T|$ and i_T as a function of tip–substrate spacing d and the concentration of R allows determination of the rate constant and the order of the reaction consuming O.

The theoretical method for treating coupled homogeneous reactions was based on the alternating direction implicit (ADI) finite difference approach that yields working curves that are fit to the experimental data.[4-6] Such curves were employed, for example, in SECM studies of hydrodimerization reactions of the activated olefins dimethyl fumarate and fumaronitrile. More recently, SECM has been used to detect the radical anion of acrylonitrile and to measure a rate constant for the anion radical dimerization of 6 (±3) × 10^7 M^{-1} s^{-1}.[7]

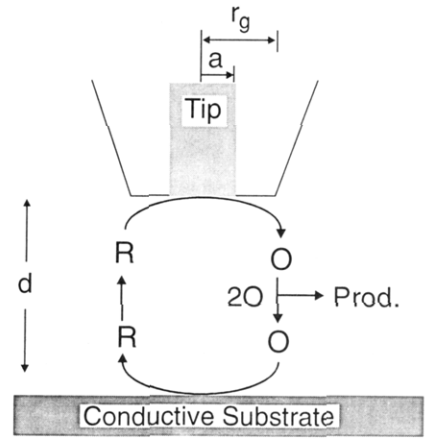

Figure 1. SECM schematic illustrating tip generation/substrate collection mode for an oxidative dimerization reaction.

The aim of this work is 2-fold: to develop an approximate analytical solution to aid in the SECM studies of first- and second-order homogeneous kinetics and to illustrate this approach while extending the range of homogeneous reactions rates which can be studied. We chose to investigate the oxidation of 4-nitrophenolate, which produces the nitrophenoxyl radical that undergoes an irreversible dimerization.[8,9] Hapiot et al. recently measured the dimerization rate constant as approximately 6.3 × 10^7 M^{-1} s^{-1} by fast-scan cyclic voltammetry.[9]

Theory

The theoretical model employed here, as earlier models, assumes that the tip and substrate potentials are such that the electron-transfer rates at both electrodes are rapid and that the homogeneous reaction is irreversible. To obtain general solutions to homogeneous kinetics by SECM, the variables were cast into dimensionless form. In the following discussion, tip and substrate currents, i_T and i_S, respectively, are normalized to the tip current at infinite tip–substrate separation (i.e., $I_T = i_T/i_{T,\infty}$ and $I_S = i_S/i_{T,\infty}$), and the tip–substrate separation, d, is normalized to the electrode radius, a ($L = d/a$).

SECM theory has been developed for two mechanisms involving homogeneous chemical reactions following electron transfer: a

† Present address: Department of Chemistry, Queens College-CUNY, Flushing, NY 11367.

® Abstract published in *Advance ACS Abstracts,* May 1, 1994.

0022-3654/94/2098-5751$04.50/0

first-order irreversible reaction (E_rC_i mechanism)[4] and a second-order irreversible dimerization (E_rC_{2i} mechanism).[5] Three approaches to kinetic analysis were proposed: (i) steady-state measurements of the feedback current, (ii) generation/collection experiments, and (iii) analysis of the chronoamperometric (i_T vs time) SECM response. Unlike the feedback mode, the generation/collection measurements included simultaneous analysis of both I_T vs L and I_S vs L curves or the use of the collection efficiency parameter I_S/I_T, when the tip is a generator and the substrate is a collector. Chronoamperometric measurements are possible but less convenient.[6]

Previously, the theory for both first- and second-order mechanisms was presented in the form of families of working curves involving two parameters.[4,5] These curves were obtained by numerical solution of partial differential equations and represent the steady-state tip current or collection efficiency as functions of a dimensionless kinetic parameter, K = const·k_c/D, and L. We present here some generalizations of the theory along with analytical approximations for the working curves. To understand this approach, it is useful to consider first the case of positive feedback with a simple redox mediator (i.e., without homogeneous chemistry involved) and with both tip and substrate processes under diffusion control.

The normalized steady-state tip current can be represented as a sum of two terms:

$$I_T = I_f + I_T^{ins} \tag{4}$$

where I_f is the feedback current coming from the substrate and I_T^{ins} is the current due to the diffusion of the electroactive species to the tip from the bulk solution taking into account how the presence of the substrate electrode blocks or hinders diffusion to the tip. I_T, the tip current with a conductive substrate, can be computed from eq 5,

$$I_T = i_T/i_{T,\infty} = 0.78377/L + 0.3315\exp(-1.0672/L) + 0.68 \tag{5}$$

$$I_T^{ins} = 1/(0.15 + 1.5358/L + 0.58\exp(-1.14/L) + 0.0908\exp[(L-6.3)/(1.017L)]) \tag{6}$$

and I_T^{ins}, the tip current with an insulating substrate, can be computed from eq 6.[10] The substrate current can be written

$$I_S = I_f + I_d \tag{7}$$

where I_f is the same quantity as in eq 4, representing the reduced species that eventually arrives at the tip as a feedback current, and I_d is the dissipation current, i.e., the flux of species from the substrate not reaching the tip. Previous simulations indicated that the collection efficiency I_S/I_T is greater than 0.99 at $0 < L \leq 2$, i.e., for any L within this interval $I_T \approx I_S$. Thus, from eqs 4 and 7

$$I_d = I_T^{ins} \tag{8}$$

or

$$I_d/I_S = I_T^{ins}/I_T = f(L) \tag{9}$$

where $f(L)$ can be computed for any L as the ratio of the right hand side of eq 6 to that of eq 5. Equation 9 implies that the ratio of the two components of I_S, I_d, and I_f, are functions only of the tip–substrate geometry, and hence L:

$$I_f/I_d = [1 - f(L)]/f(L) \tag{10}$$

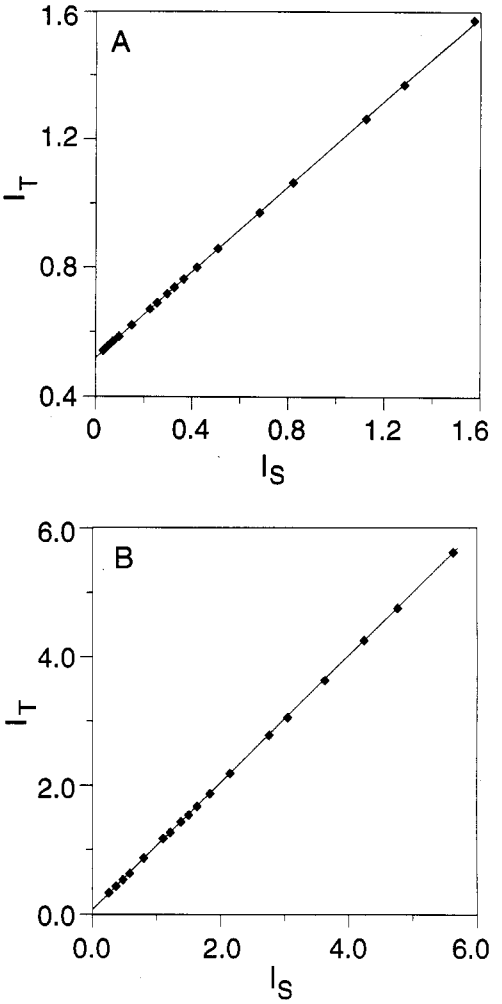

Figure 2. Tip current as a linear function of the substrate current at constant L for E_rC_{2i} mechanism. Plotted points are simulated data, taken from ref 5, for normalized rate constants from $K = 0$ to $K \rightarrow \infty$ ($K = k_c a^2 c^*/D$). (A) $L = 1$. Slope and intercept values found from the best linear fit are 0.66 and 0.52, respectively; the corresponding values computed from eqs 13, 5, and 6 are 0.66 and 0.53. (B) $L = 0.158$. Slope and intercept values are 0.98 and 0.07, respectively, and the computed values are 0.98 and 0.10.

Analogously, for an electrochemical process (e.g., an oxidation) followed by an irreversible homogeneous reaction of any order, eqs 1–3, one can write

$$I_T' = I_f' + I_T^{ins} \tag{11}$$

$$I_S' = I_f' + I_d' \tag{12}$$

where the variables labeled with the prime are the normalized tip and substrate currents in the presence of the homogeneous reaction, analogous to unlabeled variables in eqs 4 and 7. I_T^{ins}, which represents the diffusion of R to the tip from bulk solution, is unaffected by the occurrence of the homogeneous reaction in eq 3. Since species R is stable, the fraction of this species generated at the substrate and arriving at the tip should also be unaffected by the homogeneous reaction in eq 3. In other words, whatever amount of species O reaches the substrate is immediately converted to stable species R, and the flux of R from the substrate still divides into its component parts according to eq 10. Thus, the relation $I_d'/I_S' = f(L)$ still holds true. Consequently

$$I_T' = I_T^{ins} + I_S' - I_d'$$

$$I_T' = I_T^{ins} + I_S'[1 - f(L)] \tag{13}$$

Thus, for an SECM process with a following homogeneous chemical reaction of any order, a plot of I_T' vs I_S' at any given L should be linear, with a slope equal to $1-f(L)$ and an intercept equal to I_T^{ins}. The generation/collection mode of the SECM (with tip electrode serving as generator) for these mechanisms is completely equivalent to the feedback mode, and any quantity, I_T', I_S', or I_S'/I_T', can be calculated from eq 13 for a given L, if any of the other quantities is known. To check the validity of the approximation given by eq 13, we used the data simulated for an E_rC_{2i} mechanism[5] and plotted I_T' vs I_S' for different values of k_c at a given L (Figure 2). Clearly, for both intermediate ($L = 1$) and small ($L = 0.158$) distances, the I_T' vs I_S' dependencies are linear, and the slope and intercept values are in agreement with those computed from eqs 13, 5, and 6.

For the mechanisms with following irreversible reactions, one can expect the collection efficiency I_S'/I_T' to be a function of a single kinetic parameter κ. If this parameter is known, the SECM theory for this mechanism can be reduced to a single working curve. After the parameter κ is specified, one can immediately evaluate the rate constant from experimental I_S'/I_T' vs L or I_T' vs L curves. If only tip current has been measured, the collection efficiency can be calculated from eq 13:

$$I_S'/I_T' = (1 - I_T^{ins}/I_T')/[1 - f(L)] \qquad (14)$$

For a first-order irreversible homogeneous reaction, the concentration of a reactant decreases exponentially with time ($c/c^* = \exp[-k_c t]$). Thus, the collection efficiency should be a function of the dimensionless quantity $k_c t$. Under SECM conditions, the time required for an electroactive species to cross the gap between generator and collector electrodes is proportional to d^2/D, independent of a.[11] Therefore, I_S'/I_T' can be given in terms of the single-valued dimensionless parameter $\kappa = k_c d^2/D$ as an alternative to the parameter $k_c a^2/D$.[4] Figure 3A gives the working curve κ vs I_S'/I_T', along with the simulated data.[4] The numerical results fit the analytical approximation

$$\kappa = F(x) = 5.608 + 9.347\exp(-7.527x) - 7.616\exp(-0.307/x) \qquad (15)$$

(solid curve in Figure 3A), where $x = I_S'/I_T'$ within about 1%. The collection efficiency values most suitable for determination of k_c are those between about 0.2 and 0.8.

For the E_rC_{2i} mechanism the choice of κ is not straightforward. While the parameter $c^*k_c d^2/D$ appears to be the natural choice, the collection efficiency is not a single-valued function of this parameter, probably because of the nonuniform distribution of redox species within the tip–substrate gap. We found empirically that $\kappa = c^*k_c d^3/aD$ can be used to obtain an acceptable fit for the data points computed in ref 5 (Figure 3B). These data fit eq 16:

$$\kappa = 104.87 - 9.948x - 185.89/x^{1/2} + 90.199/x + 0.389/x^2 \qquad (16)$$

Although this approximation is less accurate than eq 15, its use does not lead to an error of more than 5–10%, which is within the usual range of experimental error for the determination of rate constants of rapid reactions. The rate constants calculated from data points corresponding to $0.3 \le I_S'/I_T' \le 0.9$ are most reliable. The invariability of k_C computed from different experimental points confirms the validity of this approach.

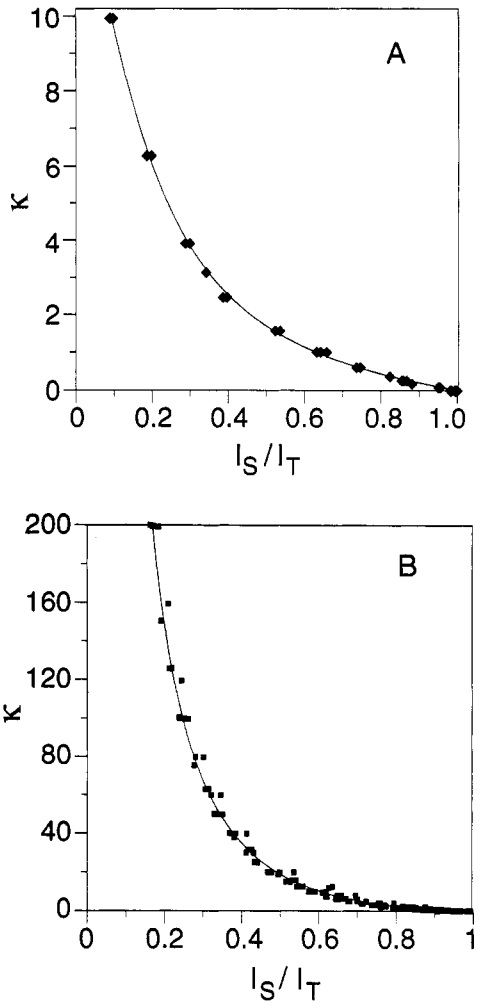

Figure 3. Kinetic parameter κ as a function of the collection efficiency I_S'/I_T'. (A) E_rC_i mechanism. $\kappa = k_c d^2/D$; solid line was computed from eq 15, and triangles are simulated data taken from ref 4. (B) E_rC_{2i} mechanism. $\kappa = c^*k_c d^3/aD$; solid line was computed from eq 16, and squares are simulated data taken from ref 5.

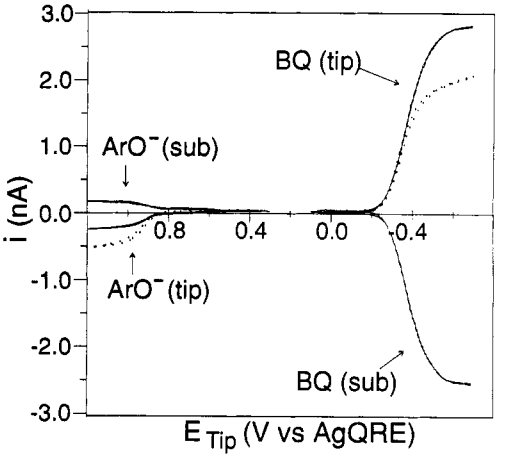

Figure 4. Representative SECM cyclic voltammograms of 4-nitrophenolate (ArO^-) and benzoquinone (BQ) taken in tip generation/substrate collection mode. The tip was scanned at 100 mV/s while the substrate potential was held constant at 0.0 V vs AgQRE. Experimental parameters are [ArO^-] = 0.40 mM, [BQ] = 20 mM. Cyclic voltammograms are shown for very large tip–substrate separation (dotted line) and 3.9-μm separation (solid line).

Experimental Section

Reagents. UV-grade acetonitrile (B&J Brand, Baxter Diagnostics Inc., McGaw Park, IL) was used as received. The supporting electrolytes, Bu_4NBF_4 and Bu_4NPF_6 (SACHEM, Austin, TX), were twice recrystallized prior to use. 4-Nitrophenol, benzoquinone, and ferrocene (Aldrich) were purified by vacuum sublimation prior to use. The base $Me_4NOH{\cdot}5H_2O$ (Aldrich) was used as received. The 4-nitrophenol was deaerated with Ar prior to stoichiometric conversion to 4-nitrophenolate with 0.50 M Me_4NOH in H_2O.

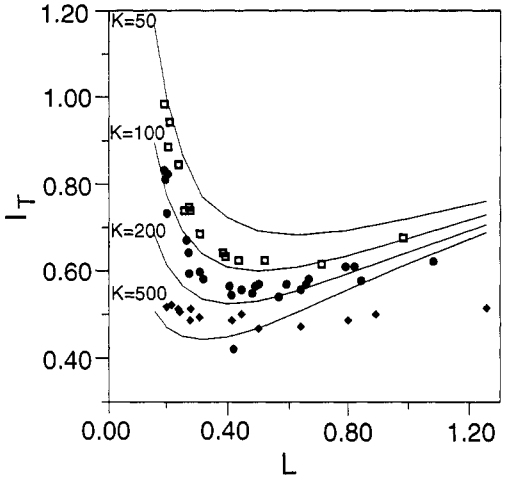

Figure 5. Normalized tip (feedback) current–distance behavior for [4-nitrophenolate] = 0.20 mM (□), 0.40 mM (●), and 0.71 mM (◆). Solid lines are dimensionless rate constants, K, from simulations in ref 5. Internal reference couple, BQ.

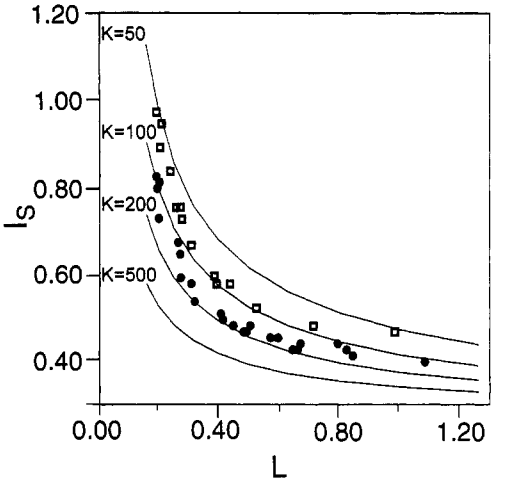

Figure 6. Normalized substrate (collection) current–distance behavior for experiment in Figure 5.

Electrodes. Ultramicroelectrode tips were fabricated from 5-μm-diameter gold wires (Goodfellow Metals, Cambridge, UK), as previously described.[12] For each tip electrode, the surrounding glass sheath was ground to yield a cone. The electrode/glass radius ratio, RG = r_g/a, varied from 2 to 5. The substrate electrode was either a 50- or 500-μm-diameter Pt wire sealed in a glass sheath. Both the tip and the substrate electrodes were polished with 0.05-μm alumina (Buehler, Ltd., Lake Bluff, IL) prior to use. Au was chosen for the tip electrode because the oxidation products of phenolates do not foul the Au surface as severely as they do Pt. A Pt wire was used as the counterelectrode and a Ag wire served as a quasi-reference electrode (AgQRE).

Apparatus. A four-electrode potentiostat (El-400, Ensman Instruments, Bloomington, IN) was used for independent control of the tip and substrate potentials. Other details of the SECM instrument have been described.[1,2,12,13]

Results and Discussion

The SECM was used to measure the homogeneous rate constant for the dimerization of 4-nitrophenolate (ArO^-) in acetonitrile. The reaction scheme for this SECM study is

$$\text{tip:} \qquad ArO^- - e \rightarrow ArO^\bullet \qquad (17)$$

$$\text{gap:} \qquad 2ArO^\bullet \rightarrow (ArO)_2 \qquad (18)$$

$$\text{substrate:} \qquad ArO^\bullet + e \rightarrow ArO^- \qquad (19)$$

Data were collected using the SECM in the tip generation/substrate collection mode (TG/SC). In this mode of operation, the 4-nitrophenoxyl radical electrogenerated at a microelectrode tip can follow two paths: reduction at the substrate electrode or reaction in the gap to form an electroinactive species prior to reaching the substrate. The 4-nitrophenolate which is regenerated at the substrate is fed back to the tip. The measured cathodic current at the substrate (collection current) and the anodic tip current (feedback current) are functions of both the electrode separation, d, and the homogeneous reaction rate in the gap, k_C. The SECM reaction scheme for the oxidation and subsequent dimerization of 4-nitrophenolate is illustrated in Figure 1.

Generally, current versus distance measurements are made by stepping the tip to a potential at which diffusion-limited steady-state currents occur. The tip is then moved toward or away from the substrate with a calibrated piezo or inchworm positioner while the steady-state substrate current is measured. This procedure was not possible for phenolate studies because side reactions led to polymers that deposited on the electrode surface, causing the tip to foul. To minimize fouling of the tip electrode, independent cyclic voltammograms were obtained at various tip–substrate separations.

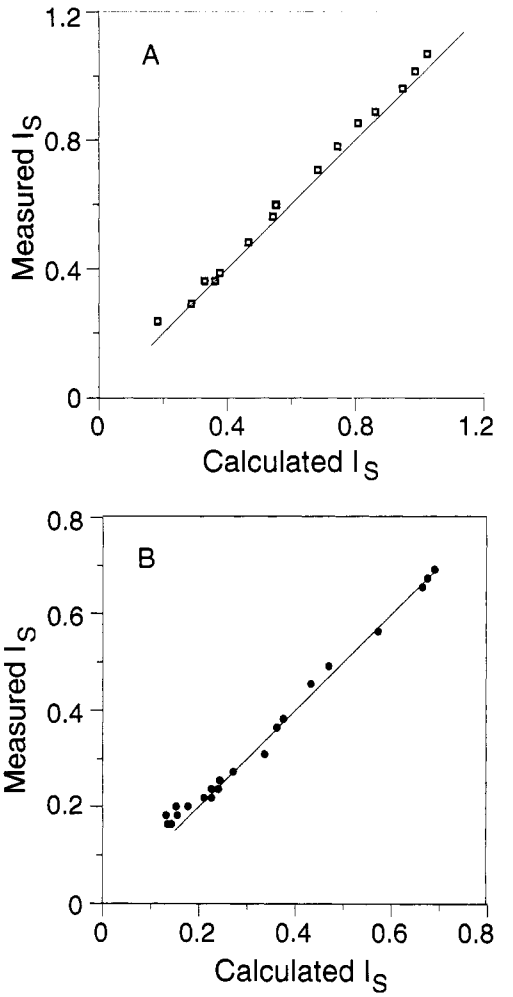

Figure 7. Comparison of the measured substrate current values (squares) to those calculated from the tip current (Figure 5) according to eq 14. c^* = (A) 0.20 mM and (B) 0.41 mM.

Although the piezo and inchworm positioners enable the tip to be moved precise distances, an internal reference species is necessary to determine the actual tip–substrate separations accurately. Benzoquinone and ferrocene were used as internal standards in this study. The relationship between SECM feedback currents and tip–substrate separation for couples with stable products follows eq 5.

TABLE 1: Calculated Dimerization Rate Constants for Various 4-Nitrophenolate Concentrations with Benzoquinone as Internal Mediator

c^*, mM	0.2[a]	0.2[b]	0.4[a]	0.4[b]	0.71[a]
k_c, 10^8 M^{-1} s^{-1}	1.4 ± 0.3	1.0 ± 0.3	1.2 ± 0.3	1.0 ± 0.2	1.3 ± 0.2

[a] From I_S'/I_T' and eq 14. [b] From fitting of working curves.[5]

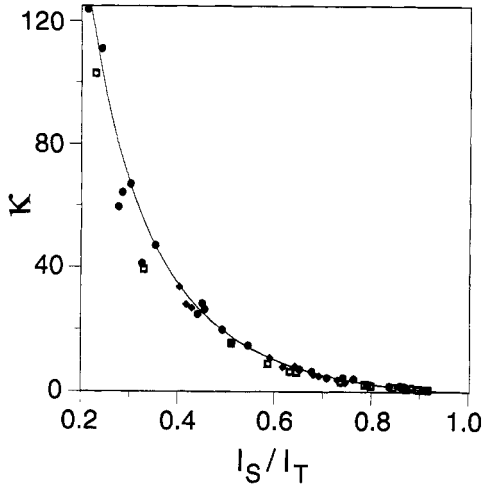

Figure 8. Kinetic parameter κ as a function of the collection efficiency. Squares were calculated from experimental data in Figure 5 with k_c = 1.2×10^8 M^{-1} s^{-1}, and solid line was obtained from eq 16. Experimental conditions as in Figure 5.

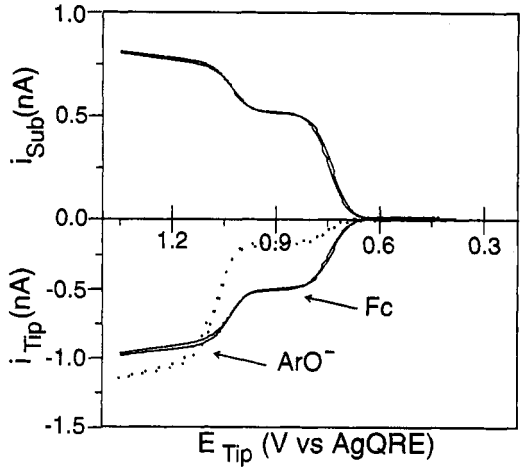

Figure 9. Representative SECM cyclic voltammograms of 4-nitrophenolate (ArO^-) and ferrocene (Fc) taken in tip generation/substrate collection mode. The tip was scanned at 100 mV/s while the substrate potential was held constant at 0.0 V vs AgQRE. Experimental parameters are [ArO] = 0.755 mM and [Fc] = 0.12 mM. Cyclic voltammograms are shown for very large tip–substrate separation (dotted line) and 1.1-μm separation (solid line).

Representative cyclic voltammograms illustrating SECM feedback and collection for 4-nitrophenolate with benzoquinone as an internal reference are shown in Figure 4. Since benzoquinone is a reducible couple, it is unreactive in the potential region where the oxidation of 4-nitrophenolate occurs. Cyclic voltammograms of both species are shown at two tip–substrate separations, $d \rightarrow \infty$ (dotted line) and 3.9 μm (solid line). As expected for a stable couple, the normalized tip current for benzoquinone increases at small separation due to positive feedback from the substrate. For 4-nitrophenolate, as predicted by theory, the anodic tip current decreases at smaller separations. The current decrease occurs for two reasons: the tip's close proximity to the substrate hinders diffusion of 4-nitrophenolate from the bulk solution, and the dimerization reaction in the gap reduces the flux of 4-nitrophenoxyl radical at the substrate, thereby reducing the feedback current.

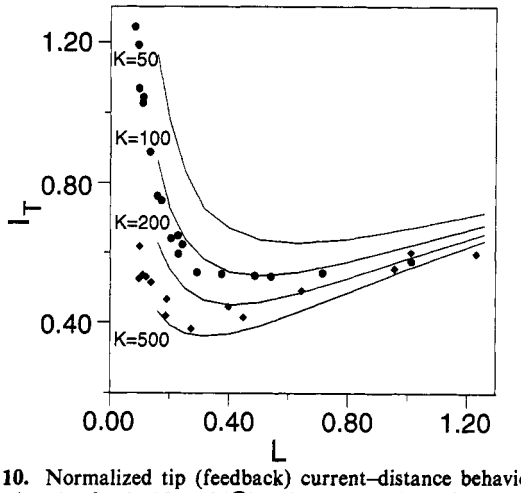

Figure 10. Normalized tip (feedback) current–distance behavior for [4-nitrophenolate] = 0.378 mM (●) and 0.755 mM (◆). Solid lines are dimensionless rate constants, K, from simulations in ref 5. Internal reference couple, Fc.

I_T vs L and I_S vs L data are plotted in Figures 5 and 6, respectively. The solid lines are simulated data for various normalized rate constants taken from ref 5 ($K = k_c a^2 c^*/D$). As tip–substrate separation decreases, the tip current initially decreases as diffusion of 4-nitrophenolate to the tip is hindered by the substrate. Substrate collection current is initially small because most of the 4-nitrophenoxyl radical reacts prior to diffusing to the substrate. The increased collection current at closer separations is also reflected in an increased tip current due to feedback. At a given electrode separation both the normalized tip and substrate currents decrease as the 4-nitrophenolate concentration is increased from 0.20 to 0.71 mM. This behavior is expected for a second-order homogeneous reaction since the reaction rate depends on concentration.

To test the consistency of the experimental data, substrate currents measured at different L for 0.20 and 0.40 mM 4-nitrophenolate (Figure 6) were compared to values calculated according to eq 14 from the I_T vs L curves (Figure 5). Agreement between the theory and experiment was within a few percent for all experimental points (Figure 7). The good agreement is strong evidence that the calculated tip–substrate separations were accurate. Furthermore, the results indicate that undesired side reactions, such as polymerization onto either electrode, are not significant.

The average values of k_c computed from eq 16 for different bulk concentrations of 4-nitrophenolate are summarized in Table 1. Two values of k_c were calculated for concentrations of 0.20 and 0.40 mM: one from the collection efficiency data obtained by dividing the measured substrate current by the tip current measured for the same L, the second by transforming the measured I_T' to I_S'/I_T' according to eq 14. No substrate current data was obtainable for the 0.71 mM solution. It can be seen from Table 1 that k_c determined at various tip–substrate separations remained constant, within an experimental error of about 30%, and independent of c^*. The average value of the dimerization rate constant computed from all experimental data points was k_c = $1.2\ (\pm 0.3) \times 10^8$ M^{-1} s^{-1}. Assuming that this is an accurate value of the rate constant, κ values were computed for all experimental points presented above and were plotted for comparison with the theoretical working curve (Figure 8). Reasonable agreement between theory and experiment can be seen, with point scatter of no more than ±20%.

Studies were undertaken to determine if the oxidative dimerization rate of 4-nitrophenolate could be similarly measured using the oxidative couple ferrocene/ferrocenium (Fc/Fc^+) as an internal reference. Typical cyclic voltammograms illustrating SECM feedback are shown for 4-nitrophenolate and ferrocene in Figure 9. Ferrocene has several disadvantages to benzoquinone

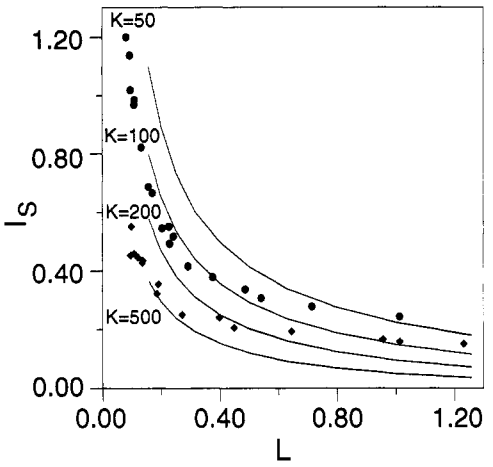

Figure 11. Normalized substrate (collection) current–distance behavior for experiment in Figure 10.

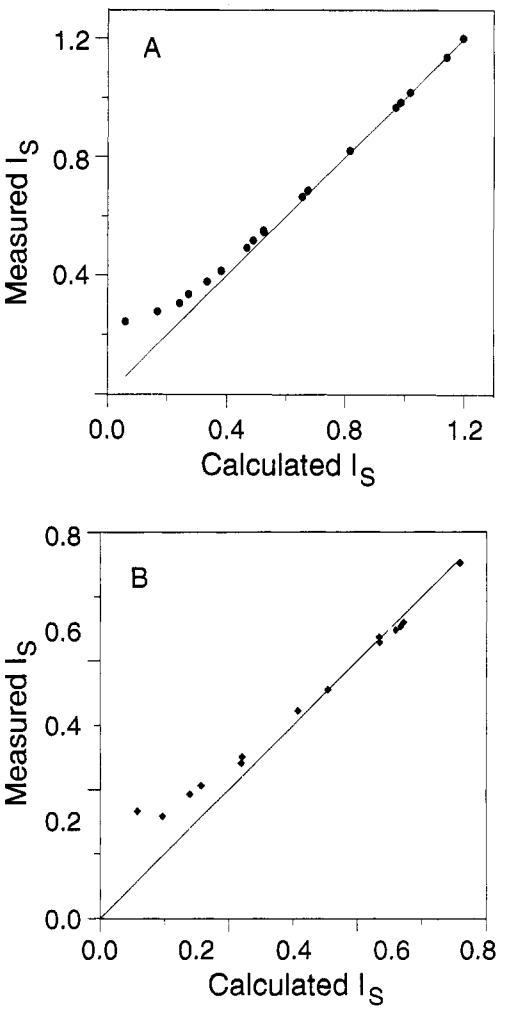

Figure 12. Comparison of the measured substrate current values (squares) to those calculated from the tip current (Figure 10) according to eq 14. c^* = (A) 0.378 mM and (B) 0.755 mM.

as a reference. First, the oxidation wave for 4-nitrophenolate overlaps with that of Fc. This necessitates subtracting the Fc component when determining the steady state current for 4-nitrophenolate. More importantly, a potential side reaction

$$ArO^{\bullet} + Fc \rightleftarrows ArO^{-} + Fc^{+} \qquad (20)$$

can occur in the gap, since electrogenerated $ArO^{\bullet}$ is a better oxidant than Fc^{+}. The occurrence of this reaction would cause replacement in the gap of the unstable $ArO^{\bullet}$ with the stable Fc^{+}

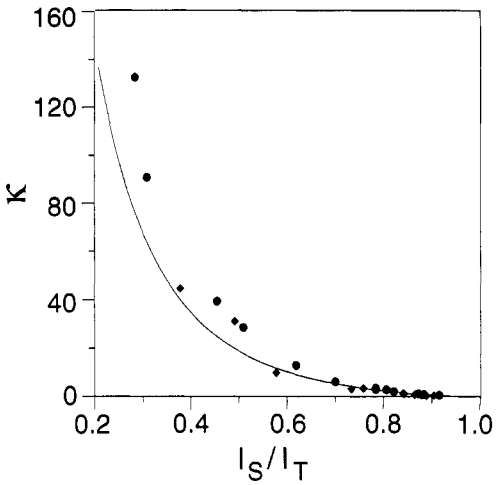

Figure 13. Kinetic parameter κ as a function of the collection efficiency. Squares were calculated from experimental data in Figure 10 with k_c = 1.5×10^8 M^{-1} s^{-1}, and the solid line was obtained from eq 16. Experimental conditions as in Figure 10.

TABLE 2: Calculated Dimerization Rate Constants for Various 4-Nitrophenolate Concentrations with Ferrocene as Internal Mediator

c^*, mM	0.378[a]	0.378[b]	0.755[a]	0.755[b]
k_c, 10^8 M^{-1} s^{-1}	1.2 ± 0.2	0.7 ± 0.3	1.8 ± 0.6	1.5 ± 1.2

[a] From I_S'/I_T' and eq 14. [b] From fitting of working curves.[5]

and would be expected to increase the collection efficiency compared to that in the absence of Fc. I_T vs L and I_S vs L data are plotted in Figures 10 and 11, respectively. Although the current vs distance behavior appears similar to the benzoquinone-mediated studies, there are more significant deviations, most notably at the largest tip–substrate separations. The deviations are bigger for the substrate current.

The measured I_S' and the value calculated using I_T' and eq 14 are in relatively good agreement at small tip–substrate separations (high collection efficiencies) but deviate as the separation is increased (Figure 12). This discrepancy between measured and calculated current values is not due to an error in measuring the tip–substrate separation. Since the oxidation of 4-nitrophenolate occurs at more positive potentials than Fc, it should have no effect on the tip and substrate currents for Fc oxidation used to determine d. It is probably the occurrence of the Fc–$ArO^{\bullet}$ reaction (eq 20), which leads to an increase in the measured substrate current, that causes the deviation. The average values of k_c computed from eq 16 for different bulk concentrations of 4-nitrophenolate with Fc as a reference are summarized in Table 2. The k_c values determined from experimental I_S' are lower than the respective ones determined from I_S' values calculated from eq 14. The Fc–$ArO^{\bullet}$ reaction (eq 20) should not affect I_T' as much as I_S' because the reaction exchanges one stable reductant, Fc, for another, ArO^{-}. However, since feedback and collection currents are intimately connected, calculations using theoretical values of substrate current are also of questionable validity. This is reflected in a plot of κ vs I_S'/I_T', using I_S' calculated from eq 14, where κ deviates from theory for $I_S'/I_T' < 0.6$ (Figure 13).

Conclusions

Analytical approximations to the simulated working curves previously presented for studying E_rC_i and E_rC_{2i} mechanisms have been developed. The approximations reduce the theoretical two-parameter working curves to a single curve. For mechanisms with following irreversible reactions, the SECM collection efficiency I_S/I_T is found to be a function of a single kinetic parameter κ. The analytical solutions have been shown to fit the simulated data for E_rC_i and E_rC_{2i} reaction mechanisms with good

accuracy. The high level of agreement between the solution for E_rC_{2i} reactions and the experimental results for 4-nitrophenolate demonstrates the usefulness of this model for measuring fast reaction rates. This is the first study which has demonstrated that the SECM is capable of measuring second-order reaction rates with rate constants greater than 10^8 M^{-1} s^{-1}. Finally, this study demonstrates that the choice of an independent mediator for measuring tip–substrate separations is important. Mediators should be chosen that will not interfere with the reaction being measured.

Acknowledgment. The support of this work by grants from the National Science Foundation (CHE 9214480) and the Robert A. Welch Foundation is gratefully acknowledged.

References and Notes

(1) Bard, A. J.; Fan, F.-R. F.; Kwak, J.; Lev, O. *Anal. Chem.* **1989**, *61*, 132.
(2) Bard, A. J.; Fan, F.-R. F.; Mirkin, M. V. In *Electroanalytical Chemistry*, Bard, A. J., Ed.; Marcel Dekker: New York, 1994; Vol. 18, p 243.
(3) Bard, A. J.; Fan, F.-R. F.; Pierce, D. T.; Unwin, P. R.; Wipf, D. O.; Zhou, F. *Science* **1991**, *254*, 68.
(4) Unwin, P. R.; Bard, A. J. *J. Phys. Chem.* **1991**, *95*, 7814.
(5) Zhou, F.; Unwin, P. R.; Bard, A. J. *J. Phys. Chem.* **1992**, *96*, 4917.
(6) Unwin, P. R.; Bard, A. J. *J. Phys. Chem.* **1992**, *96*, 5035.
(7) Zhou, F.; Bard, A. J. *J. Am. Chem. Soc.* **1994**, *116*, 393.
(8) Evans, D. H.; Jimenez, P. J.; Kelly, M. J. *J. Electroanal. Chem.* **1984**, *163*, 145.
(9) Hapiot, P.; Pinson, J.; Yousfi, N. *New J. Chem.* **1992**, *16*, 877.
(10) Mirkin, M. V.; Fan, F.-R. F.; Bard, A. J. *J. Electroanal. Chem.* **1992**, *328*, 47.
(11) Mirkin, M. V.; Arca, M.; Bard, A. J. *J. Phys. Chem.* **1993**, *97*, 10790.
(12) Wipf, D. O.; Bard, A. J. *J. Electrochem. Soc.* **1991**, *138*, 469.
(13) Kwak, J.; Bard, A. J. *Anal. Chem.* **1989**, *61*, 1794.